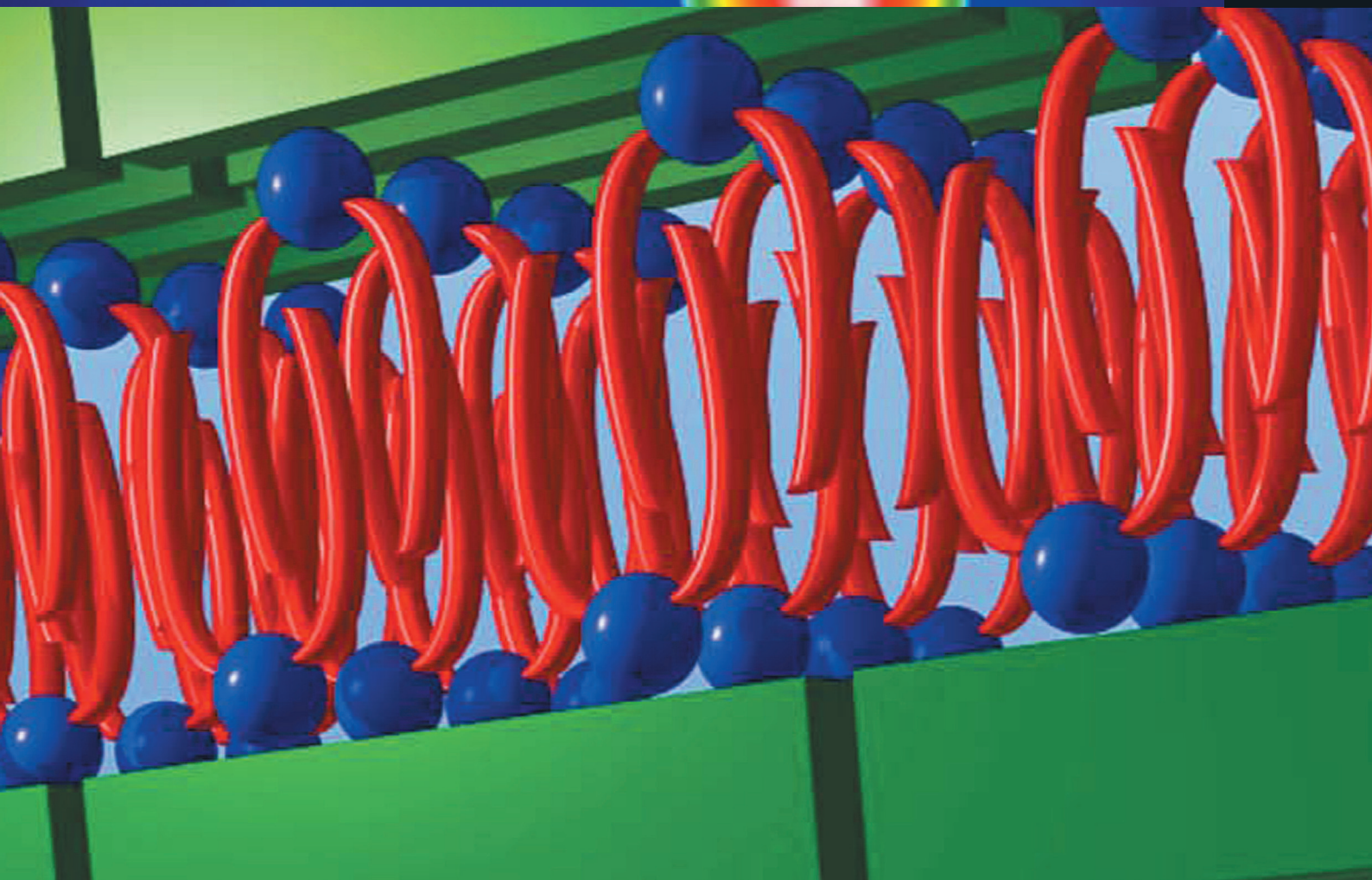


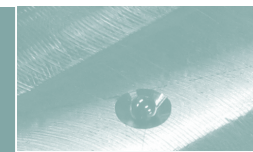
XMAS

NEWSLETTER

2012



CONTENTS



4 Grant Announcements

5 Condensed Matter

6 Surfaces & Interfaces

7 Cultural Heritage

8 Soft Matter

10 Theory

11 Guidelines

On the cover: ordered lamellar structure of an organic nanofilm (bottom image, see article p. 9) and reciprocal space map showing antiferrodistortive order (top image, see article p. 5).

It brings us very great pleasure to present the XMaS newsletter in what has now become the 4th operational phase of the beamline project!

Following detailed negotiations and a number of written submissions to EPSRC and BIS, we are pleased to announce that the XMaS beamline is to be supported as an EPSRC «mid-range facility» for the period 2012-2017 (see the message written by our EPSRC representative Simon Crook on page 4). Full details of XMaS and the other mid-range facilities can be found on the EPSRC website (www.epsrc.ac.uk).

Operation as a «mid-range facility» is slightly different to the previous «responsive mode» operations, as the beamline is now run under a service contract between the EPSRC and the Universities of Liverpool and Warwick. Part of this contract includes Key Performance Indicators to monitor output on a 6 month cycle and these will be available on our new (and evolving) webpage <http://www.xmas.ac.uk>. It is thus vital that you, our Users, keep us informed of publications and any other output that results from the experiments that are performed on the beamline. In agreement with EPSRC, a review of the beamline and its operations will be conducted in 2015. This will then determine if there will be life beyond 2017: please help us by continuing to publish results in high quality journals!

Last May, the beamline was reviewed by the ESRF Science Advisory Committee (SAC). The comments of the Review Panel were very positive and supportive. They recognised the strength and diversity of the research conducted on the beamline. The panel highlighted the strength in studying resonant scattering in correlated electron systems, particularly at the 4d L edges. They encouraged further efforts in the field of soft matter and interface science as well as strongly supporting the expansion of the low energy capability towards 2 keV, with parallel development of appropriate sample environments. In partnership with our Users, these recommendations will

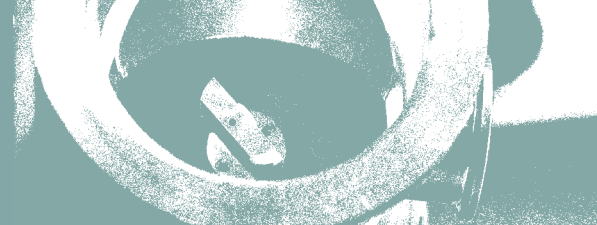
help shape the future direction of XMaS and we encourage you to get in touch with any new ideas or opportunities that we can help to realise.

We will highlight the latest technical developments and scientific output at our next User meeting which will be held at the University of Liverpool on 15th May 2013. Please reserve this date in your diaries and come along. If you are thinking of using the beamline this is an excellent opportunity to meet the team and find out how it all works. We will, of course, cover travel and other ancillary expenses.

Another piece of good news is the launch of a new collaboration between XMaS and the National Physical Laboratory (NPL). NPL has recently been awarded two separate grants to develop an in-situ interferometric measurement system on the beamline. See the article by Markys Cain on page 4 for more details.

An identified highlight of the XMaS project has been its commitment to training the next generation of synchrotron radiation (SR) users and materials scientists. Although our statistics are incomplete, we have trained over 160 PhD students and over 45 PDRAs some of whom have been supported through EPSRC and EU supported training networks. The design of the beamline is not complicated and even inexperienced users can be trained rapidly in its basic operational modes. If you run an existing Centre for Doctoral Training (CDT) or are planning a new CDT application this year and believe that XMaS could serve as part of the training within the CDT, then please contact the project directors, Chris Lucas and Tom Hase, to discuss this in further detail.

In the current operating cycle we will continue to offer flexibility in involving new user communities and developing tailored sample environments for new scientific challenges. Being based on a bending magnet x-ray source, means that the beamline delivers a broad x-ray beam with



a low power density that is ideal for the study of materials sensitive to beam damage or at low temperatures. For example, a new optical microscope to observe x-ray excited light from materials is being developed to study the spatial variations in materials without the need for nano-focused beams with high power density. It has also been demonstrated that the implementation of combined high magnetic and electric fields, coupled with low temperatures, is changing the understanding of the fundamental processes occurring in multiferroic and magnetic materials leading to new technological devices. Recent developments at lower x-ray energies (sub 3 keV including the sulphur K (2.47 keV) and potentially the phosphorus K (2.145 keV) edges), open up unique opportunities for scattering studies of biomaterials and functional organics. If you have an idea for an experiment that can make use of the XMaS beamline but requires some instrumental development in terms of sample environment then please don't hesitate to contact us, as funds may be available for such projects.

In the near future we also plan to implement a «Rapid Access» scheme available to EPSRC major grant holders to explore whether XMaS can become a tool for any part of their research programme. Please let us know if this may be of interest to you.

The development of complex instrumentation for performing SR experiments means that there is now a suite of experimental equipment that forms part of the mid-range facility that can be used without the SR beam, i.e. can be used off-line. For example, it is possible to perform resistivity and electrical polarisation (PE) loops in a range of sample environments exploiting our different magnets: using the 4 T superconducting magnet, ± 2 kV can be applied to a sample over the temperature range 2–320 K. Alternatively, the 1 T electromagnet, which can be reversed rapidly, allows ± 10 kV to be applied in cryostats which cover the temperature ranges 10–320 K and soon to be extended to 800 K. In addition we are currently finalising the plans to develop a stand-alone x-ray facility, adjacent to the beamline. It will use a micro-focus Cu x-ray source and a 4-circle Huber diffractometer that accommodates the same range of sample environments that are available on the beamline. This will facilitate sample alignment and preparation for beamline experiments, but may also be used independently. Coupled with access to other facilities at the ESRF and on the wider EPN campus, there will be certain cases where support experiments could be performed without access to the SR beam. We are pleased to announce that we have some additional funds to support a small number of users to make use of these facilities. Please contact us for more details if you think

you may be interested in using them, as the SR beamline takes priority on any equipment and staff resources.

In the changeover to the new operational phase there have been no significant changes in the beamline personnel based in Grenoble. Simon Brown (sbrown@esrf.fr) is the Beamline Responsible who, in partnership with the Directors, oversees the activities of the user communities as well as the programmes and developments that are performed on the beamline. Laurence Bouchenoire (boucheno@esrf.fr) is in charge of Beamline Operations and can provide you with general information about the beamline, application procedures, scheduling etc. Simon Brown, Oier Bikondoa (oier.bikondoa@esrf.fr), Didier Wermeille (didier.wermeille@esrf.fr) and Laurence Bouchenoire are Beamline Scientists and will provide local contact support during experiments. They can also assist with queries regarding data analysis and software. Paul Thompson (pthomps@esrf.fr) is the contact for instrument development and technical support. He is assisted by John Kervin (jkervin@liv.ac.uk) who is based at Liverpool but spends part of his time on-site at XMaS. The Project Directors, Chris Lucas (clucas@liv.ac.uk) and Tom Hase (t.p.a.hase@warwick.ac.uk) continue to travel between the UK and France to oversee the operation of the beamline. Malcolm Cooper (m.j.cooper@warwick.ac.uk) remains involved in the beamline operation as an Emeritus Professor at the University of Warwick.

XMaS will continue to support up to 3 users per experiment at a new improved **per diem of €70**. For experiments which are user intensive, additional support may be available. Do remember to complete the «A-form» when requested to by the ESRF, as this is used for hostel bookings, site passes and to inform the safety group of attendees. The administration for XMaS has passed into capable new hands! India Foster (i.e.foster@warwick.ac.uk) is now the principal administrator on the project and is based in the Department of Physics at Warwick. All queries regarding expenses claims, etc should be directed to her. Linda Fielding (linda.fielding@liv.ac.uk) is the administrator at the University of Liverpool. We would like to thank Sandra Beaufoy at Warwick for her many years of service in administering the beamline. Sandra will continue to attend the meetings of the Project Management Committee in an advisory capacity.

Chris Lucas, Tom Hase and Malcolm Cooper

A few words from EPSRC

EPSRC has funded the XMaS beamline for over fifteen years and is pleased to announce further funding for another five years. For a group to maintain large scale grant funding for this time speaks volumes of the quality of science from the community who use the facility, the in-house programmes and the management of XMaS.

The output of the beamline in terms of papers and equipment design has impressed not just the all-important peer review but also senior research council staff who have visited ESRF and spoken to the in-house research team. I would like to encourage more people to think about using XMaS now that the funding is secured for another five years.

I have personally been the contact at EPSRC for the facility some years ago whilst in the physics programme at EPSRC, and was pleased to find myself back as the contact point at EPSRC this year. I look forward to seeing how the facility can support more world class research and encourage it to become well known throughout the UK scientific community.

*Simon Crook (Senior Manager,
Physical Sciences, EPSRC)*

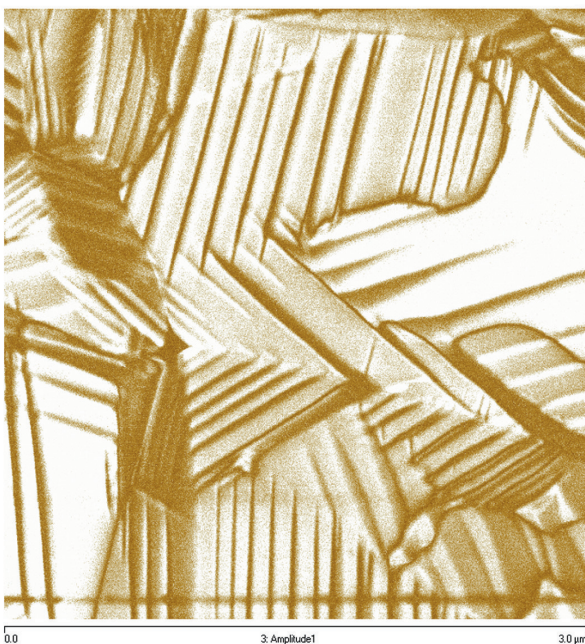


Fig. 1: Piezoresponse Force Microscopy image of the complex domain structures present in modern piezoelectric materials. Copyright NPL, 2012.

Long term research collaboration between NPL and XMaS

For more information contact Markys Cain, National Physical Laboratory, Teddington, TW11 0LW, UK.

Markys.Cain@npl.co.uk

Following the recent joint NPL/XMaS publication detailing the in-situ PE loop electrical characterisation system entitled «Simultaneous measurement of X-ray diffraction and ferroelectric polarization data as a function of applied electric field and frequency» [1], the collaboration between NPL and XMaS has been significantly strengthened. The current PE system was developed under UK National Measurement System (NMS) projects at the National Physical Laboratory (NPL). Two new applied R&D metrology projects, one funded by the European Union under the European Metrology Research Programme (EMRP 2012) and one funded by the UK's NMS (NMS-IRD), takes the collaboration to the next level – that of development of a unique in-situ interferometric measurement system to be retrofitted to the XMaS beamline.

Incorporating traceable interferometric measurements in-situ with XRD will eventually allow users of the facility to be able to correlate macroscopic measurements of piezoelectric strains of samples to their intrinsic crystallographic changes with applied electric field, temperature and magnetic field. This will be a world unique capability allowing scientists to understand the nature of the contribution of extrinsic domain wall motion (Fig. 1) to overall piezoelectric performance of new high-strain actuation and high sensitivity transducer materials currently being developed for next generation memory and electronic devices, sensors and actuators. We will be able to link the measurement of strain between up to 8 decades in length scales (tens of pm atomic displacements in mm sized samples). The new metrology capability underpins the development of novel piezoelectric electronic devices, such as the Piezoelectric-Effect-Transistor (PET) [2] under development by IBM (collaborators in this project), to enable More Than Moore strategy for faster, low power transistors.

While the NMS-IRD project is running until May 2015, the EMRP project will begin in 2013 and finish in June 2016.

[1] J. Wooldridge *et al.*, *J. Synchrotron Rad.* 19, 710 (2012).

[2] D. Newns *et al.*, *J. Appl. Phys.* 111, 085409 (2012)

Competing antiferroelectric and antiferrodistortive instabilities in EuTiO_3

J.-W. Kim, P. Thompson, P.S. Normile, J.A. Schlueter, S.D. Brown, A. Shkabko, A. Weidenkaff, P.J. Ryan – for more information contact P.J. Ryan, Advanced Photon Source, Argonne, IL 60439, USA

pryan@aps.anl.gov

The tetravalent titanate perovskite is an interesting subgroup of the emerging complex ordered oxide family. The reason is related to the underlying competition between both oxygen octahedral rotations and polar derived non-centrosymmetric B-site titanium displacements. The former generally leads to paraelectricity and the latter to ferroelectricity. Both of these phenomena are related to phonon structural instabilities. In all known cases one instability dominates. We have for the first time in a simple ABO_3 perovskite EuTiO_3 (ETO) shown that both can coexist in an exotic dynamic superstructure illustrated in **Fig. 2** [1].

In addition the rare-earth A-site, Eu^{2+} , carries a strong spin moment $\sim 7\mu_B$. ETO in bulk form is an antiferromagnet (AFM) paraelectric with $T_N \sim 5.3\text{K}$. Typically in the pseudo perovskite ferroic materials the B-site generates either polar or magnetic characteristics. Thus, the potential for both multiferroicity and magnetoelectricity comes from the A (Eu) and B (Ti) sites [2,3].

Most interestingly below T_N , ETO demonstrates a strong magneto-dielectric coupling phenomenon. As the Eu spins order, there is a $\sim 14\%$ drop in the dielectric constant and with an applied magnetic field sufficient to align the spins, the dielectric constant turns sharply up [4]. The presumption that the dielectric constant derives from the soft Ti phonon mode begs the question: are the Eu spins coupled to the Ti phonon modes? In effect the oxygen displacement order seems to mediate the Eu–Ti relationship. To understand this would allow us to potentially tap a powerful single phase magneto-electric coupling parameter.

In order to test whether the oxygen plays any role coupling the Eu 4f spins and the Ti phonon modes, we applied both electric (E) and magnetic (B) fields whilst monitoring the oxygen related half order modulations. By applying solely an E field up to $0.67 \times 10^5 \text{ V/cm}$, no effect was measured. Similarly, with only a B field

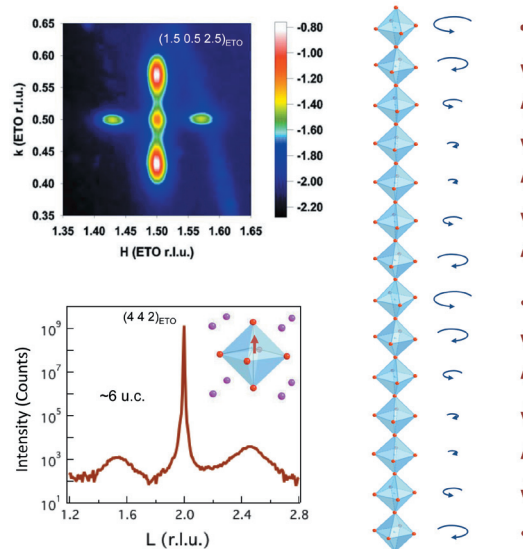


Fig. 2: (Top left) reciprocal space map typical of the AFD order due to the octahedral oxygen rotations. The satellite reflections indicate incommensurate rotational modulation domains. (Bottom left) L scan through a (442) reflection showing (0 0 1/2) order superstructure peaks related to antiferroelectric (AFE) Ti shifts coexisting with oxygen rotations. The sketch on the right summarizes the model presented with oxygen rotation (left) and Ti displacement (right).

no effect was found on the oxygen order even with fields $> 0.8 \text{ T}$ (red curve in **Fig. 3**). However when both fields were applied simultaneously the oxygen modulated intensity increased by $\sim 10\%$ (blue curve in **Fig. 3**). Our model suggests multiple orbital couplings between the intra-atomic Eu 4f-5d and interatomic O 2p and Ti 3d states. The displaced Ti atom changes the intricate electronic balance with the Eu spins by suppressing the degree of freedom of the antiferrodistortive (AFD) rotation.

- [1] J.-W. Kim *et al.*, Phys. Rev. Lett., 110, 027201 (2013).
- [2] J.H. Lee, *et al.*, Nature 466, 954 (2010).
- [3] P. J. Ryan *et al.*, Nat. Commun. 4, 1334 (2013).
- [4] T. Katsufuji, *et al.*, Phys. Rev. B 054415, (2001).

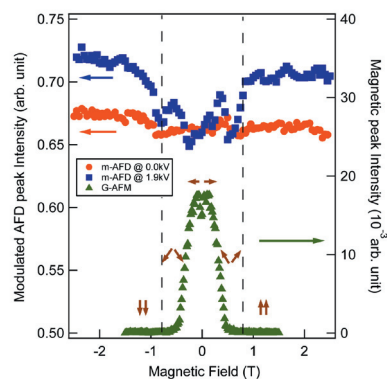


Fig. 3: Coupled B and E fields: modulated AFD intensity with (blue curve) and without (red curve) E field. AFM reflection (green curve) with suppression at $\sim 0.8\text{T}$ as the Eu spins align as illustrated by the arrows.

Direct measurements of field induced strain in magnetoelectric composites

M. Abes, C. T. Koops, S. B. Hrkac, E. Quandt, L. Bouchenoire, O. M. Magnussen and B. M. Murphy – for more information contact B. M. Murphy, Institute for Experimental and Applied Physics, University of Kiel, 24098 Kiel, Germany

murphy@physik.uni-kiel.de

A new method for determining magnetic field induced strain was investigated by means of x-ray diffraction on forbidden Bragg reflections in a magnetoelectric (ME) composite consisting of a (001) ZnO piezoelectric single crystal substrate and a $\text{Fe}_{58}\text{Tb}_{42}$ magnetostrictive amorphous layer. ME composites transform the magnetic field energy into an electric field energy or *vice versa* via elastic strain coupling at the interface between the magnetostrictive and piezoelectric components. Understanding this interface strain coupling is therefore essential to manufacture composites with a better efficiency for future sensor applications [1]. The ME effect is the product of the elastic, magnetostrictive and piezoelectric properties of the constituents, the interface coupling and the geometry. While the bulk properties and geometrical effects are well understood [2], information on the interface strain coupling is still missing. In our study,

we use the fact that the lattice deformation breaks the symmetry of the ZnO wurtzite structure allowing the appearance of forbidden reflections.

Specular reciprocal space scans measured across the (4-40) ZnO reflection were collected for pure ZnO and FeTb/ZnO (Figs 4a and b) at different distances d from the ZnO surface or FeTb/ZnO interface as depicted in the inserts of Fig. 4. The results show that the ZnO substrate is under post-deposition induced tensile strain, reaching a maximum value of $(1.1 \pm 0.1) \cdot 10^{-4}$ at the ZnO/FeTb interface. This value is very close to that measured on the (3-31) ZnO forbidden Bragg reflection (not showed here). Indeed we found that at the interface the integrated intensity of the (3-31) ZnO collected on FeTb coated on ZnO exceeds that for pure ZnO by a factor of 2 and corresponds in our calculation to an increase of the strain to about $(1.6 \pm 0.6) \cdot 10^{-4}$.

The intensity of the (3-31) ZnO was also found to increase under application of a magnetic field along the [1-10] direction (Fig. 5a). This indicates a field induced strain (ϵ_H) at the FeTb/ZnO interface (Fig. 5b). The strain approaches a nearly constant value at fields of ~ 0.05 T and exhibits a similar behavior to the saturation magnetostriction curve (λ) of the FeTb layer measured with the cantilever technique [3] (green curve in Fig. 5b).

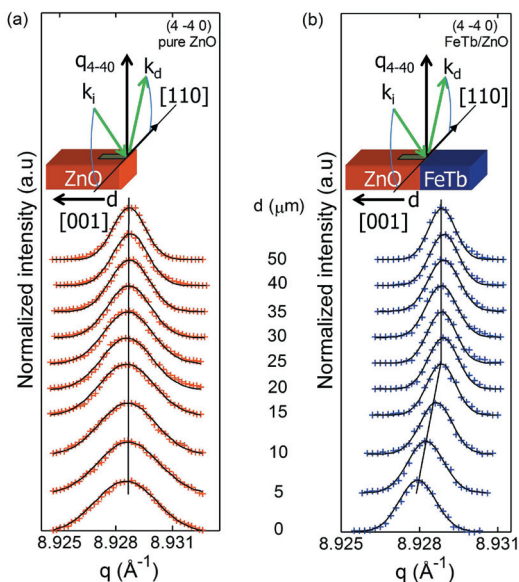


Fig. 4: (4-40) ZnO Bragg reflection measured at different positions d on pure ZnO (a) and FeTb/ZnO sample (b) with a beam size of $10 \mu\text{m}$ in the [001] direction. The solid lines result from fits with a Gaussian. All the scans have been shifted for clarity. The inserts show the schematic of the x-ray diffraction geometry.

- [1] Ce-Wen Nan *et al.*, J. Appl. Phys. 103, 031101 (2008).
 [2] J. Ma *et al.*, Adv. Mat. 23, 1062 (2011).
 [3] E.D. Delacheisserie and J.C. Peuzin, J. Magn. Magn. Mater. 136, 189 (1994).

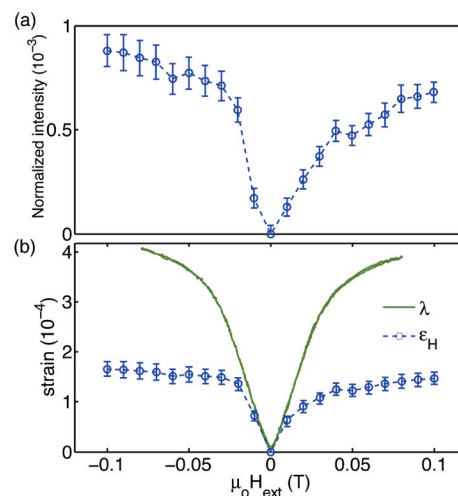


Fig. 5: (3-31) integrated intensity (a) and resulting field induced strain (ϵ_H) along the [1-10] direction (b) as a function of applied field. The magnetostriction curve λ is shown for comparison. The dashed lines are guides to the eye.

Copper corrosion - from neolithic metallurgy to synchrotron light

M. Dowsett and A. Adriaens - for more information contact M. Dowsett, Department of Physics, University of Warwick, Coventry CV4 7AL, UK or M. Adriaens, Department of Analytical Chemistry, Ghent University, Krijgslaan 281 S12, B9000, BE.

m.g.dowsett@warwick.ac.uk
annemie.adriaens@ugent.be

Humans have been using copper and its alloys for 10,000 years, but problems with the degradation of both ancient and modern artefacts through corrosion still persist. Nantokite (CuCl) acts as a precursor to other corrosion products such as paratacamite ($\text{Cu}_2(\text{OH})_3\text{Cl}$), and is often concealed under a crust of more benign material such as copper carbonate. It can weaken the metal by penetrating deeply and is unstable at high relative humidities converting to paratacamite, or cuprite (Cu_2O), for example. The latter reaction releases HCl which can further attack the copper [1]. For the conservation of copper and bronze, key questions are: do treatments designed to remove chlorides or inhibit their formation work, and how can they be tested?

Observing corrosion in real time with synchrotron x-ray diffraction (XRD) can help find the answers. On XMaS, we obtain time-lapse sequences of deliberately induced reactions as they proceed, using the MAR CCD 165 camera for fast surface diffraction. In a recently described experiment [2], we tested a protocol for forming nantokite, and described experiments to observe the process in real time

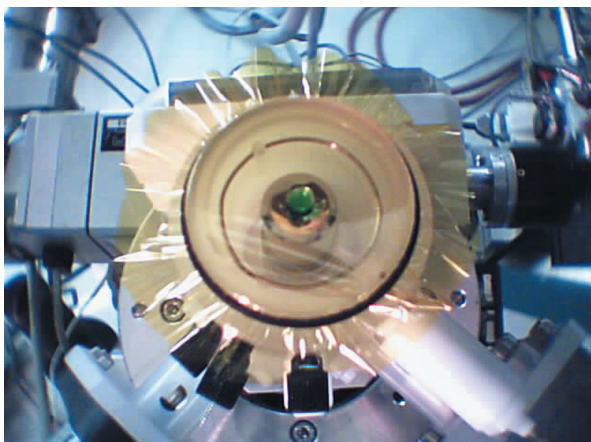


Fig. 6: eCell on XMaS just before the sample rams into a corrosive droplet. XRD is already under way.

using our eCell (electrochemical / environmental cell) [3], previously developed on XMaS and elsewhere.

The eCell contains a piston with the sample (in this case a copper disc) mounted on top. A 6 mm thick Kapton® window covers the top of the cell which would normally be filled with a gas or a liquid. The sample may be brought to within 100 μm of the window using a stepper motor under remote control. In this experiment (Fig. 6) we suspended a droplet of corrosive medium (saturated CuCl_2 solution) from the inside of the window. Once MAR acquisition had commenced, the piston was raised to squash the droplet between the copper and the window, thus distributing CuCl_2 solution over the coupon. The growth of nantokite is clearly seen in the time-lapse patterns (Fig. 7) extracted from the MAR images using our package esaProject [4]. However, its partial conversion to cuprite and paratacamite is also observed during a later rinsing stage, showing that this common protocol is unsatisfactory, but giving a further example of time-lapse chemistry.

The droplet experiment has also been used to examine the effect of water on nantokite in more detail, and to observe the formation of atacamite and paratacamite. In a similar experiment we have looked at the time lapse growth of a protective layer of lead myristate on lead in real time.

[1] D.A. Scott, "Copper and Bronze in Art: Corrosion, Colorants, Conservation", The Getty Conservation Institute, Los Angeles (2002).

[2] M.G. Dowsett *et al.*, *Anal. Chem.* 84, 4866 (2012).

[3] M.G. Dowsett, A. Adriaens, *Anal. Chem.* 78, 3360 (2006).

[4] <http://www2.warwick.ac.uk/fac/sci/physics/research/condensedmatt/sims/esaprojectpublic>

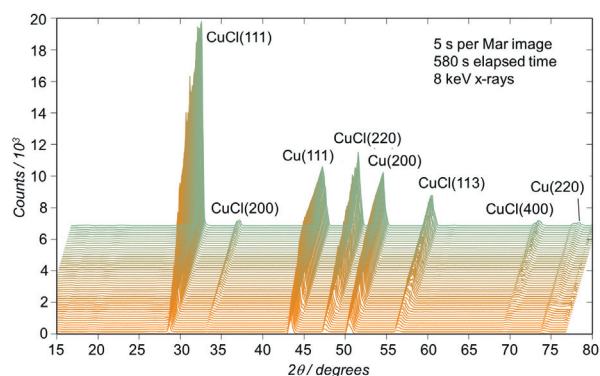


Fig. 7: Time lapse patterns showing CuCl growth.

New liquid crystals: segmented cylinders, crossed ribbons and ribbons between sheets

F. Liu, M. Prehm, X.B. Zeng, G. Ungar, C. Tschierske
– for more information contact G. Ungar, Department
of Materials Science and Engineering, University of
Sheffield, Sheffield S1 3JD, UK

g.ungar@shef.ac.uk

With sticky hydrogen-bonding groups at the ends and flexible chains attached to the side of the aromatic rods, T-shaped molecules have been found to assemble into a range of honeycomb-like structures, where the aromatic rods form the walls and the side chains fill the channels. By increasing the size of the side-chain, the shape of the polygonal cells can be changed from triangular, via rhombic, square, pentagonal, hexagonal to stretched hexagonal, as more rods are required to encircle the cell [1].

The work highlighted here [2] has gone further. Chemists at Martin Luther University in Halle have replaced the linear side chain with a branched “swallow-tail” one (Fig. 8). Their coworkers from Sheffield have found, using GISAXS at XMaS, that the honeycomb has been turned inside-out. Instead of forming the walls of the honeycomb, the aromatic rods group in bundles and form segmented columns now in the centre of the hexagonal cells. The side-chains are now on the outside, as in classic discotic columnar liquid crystals (LC).

Unlike in discotics, where birefringence is negative ($\Delta n < 0$), here $\Delta n > 0$ because the rods align parallel to the columns. There is also a weak 3D order in this structure (Fig. 8d) corresponding to space group $P6/mmm$. Furthermore, the two incompatible branches on the lateral chain, the semiperfluorinated (R_F) and the carbosilane (R_{Si}), tend to microphase separate; the R_F -rich areas are coloured blue in the electron density map in Fig. 8d, reconstructed from the powder X-ray diffraction pattern (Fig. 8a).

On decreasing the temperature, a transition to a lamellar phase takes place via an intermediate 3D orthorhombic phase with space

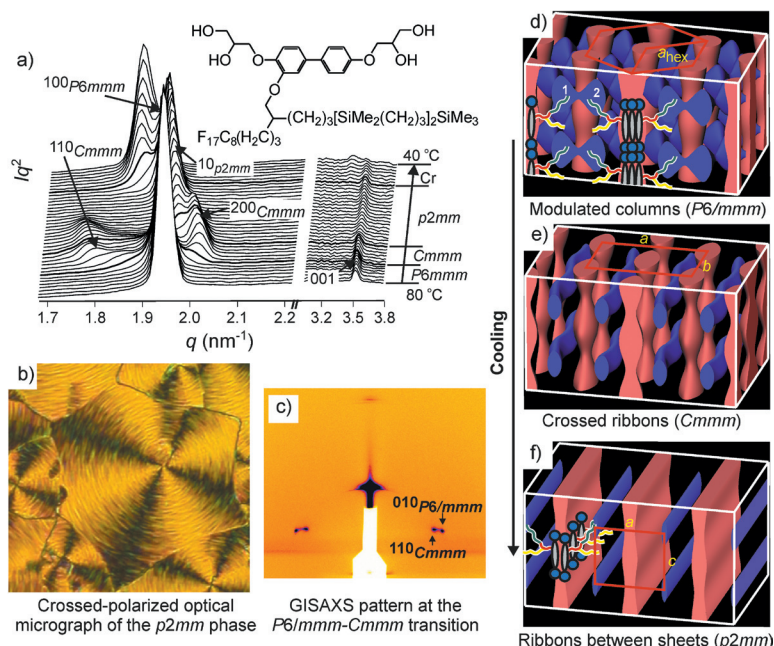
group $Cmmm$ (Figs. 8c and e). The circular columns turn to elliptical ribbons. The $Cmmm$ phase consists of two orthogonal interpenetrating sets of ribbons with the modulated ones containing aromatic rod bundles and the undulating R_F -rich ribbons. On further cooling, the aromatic ribbons fuse to form infinite sheets, while the R_F -rich ribbons straighten up. Thus, this phase features fluorinated ribbons between aromatic sheets (Fig. 8f). It has 2D long range order with plane group $2mm$. On the 10–100 μm scale the sheets roll up in scrolls giving the “CD ROM” like appearance in Fig. 8b.

In summary, three new LC phases were discovered, each with an intriguing structure: a hexagonal 3D phase with correlated modulated columns, a 3D phase with crossed ribbons and a phase with ribbons between layers. The discoveries of new and ever more complex structures show great promise of new nanomaterials for optics and molecular electronics, photovoltaics, LED, ceramics templating and other applications.

[1] C. Tschierske, Chem. Soc. Rev. 36, 1930 (2007).

[2] F. Liu *et al.*, Angew. Chem. Int. Ed. 50, 10599 (2011).

Fig. 8: The three new LC phases in the swallow-tail branched amphiphile: (a) powder SAXS traces on cooling, (b) micrograph, (c) GISAXS, (d–f) electron density maps with schematic molecules added (red – aromatic, blue – fluorinated).



Interactions of nanoparticles with purple membrane films

J.M. Bulpett, A.M. Collins, N.H.M. Kaus, P.T. Cresswell, O. Bikondoa, D. Walsh, S. Mann, S.A. Davis and W.H. Briscoe – for more information contact W.H. Briscoe, School of Chemistry, University of Bristol, Cantock's Close, Bristol BS8 1TS, UK.

wuge.briscoe@bristol.ac.uk

We increasingly look at nature for inspiration in making new materials, including for example the design of hybrid nanocomposites [1]. Lamellar structures self-assembled from purple membranes (PM) of *Halobacterium salinarum* [2] (a halophile from the archaea domain) are promising building units for bio-electronic devices, due to the proton pumping ability of the PM. The functionality and durability of such devices are hinged on the structural integrity of PM lamellae. Using X-ray diffraction, we examined the structure of PM multilayers on silicon when challenged with two types of nanoparticles (NPs): Carboxymethyl-dextran coated magnetite (Fe_3O_4 with 2.4 nm core size) and citrate-stabilised gold (5 nm core size) as depicted in Fig. 9. We tried to infiltrate the PM multilayers with the NPs using two alternative routes: facile penetration (FP) and co-assembly (CS) by solution mixing.

Films on silica were examined by X-ray reflectivity. The same technique has been used by the Bristol group to study organic semiconducting oligo (aniline) nanofilms with similarly ordered lamellar structures [3]. We found [4] that under all conditions the NPs did not disrupt the overall lamellar structure of the PM films or enter the inter-lamellar space, although the presence of NPs affected the self-assembly process of the PM films. Fig. 10 shows how the PM individual layer thickness d , the coherence length L and the number of layers m in the films ($m = L/d$) were affected by the Fe_3O_4 NPs. Both types of NPs had

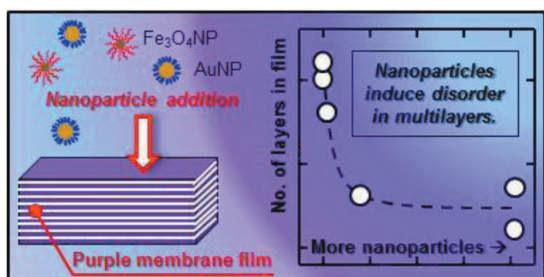


Fig. 9: Schematic showing that addition of two different types of NPs to a purple membrane film reduces the number of layers in the multilayer stack.

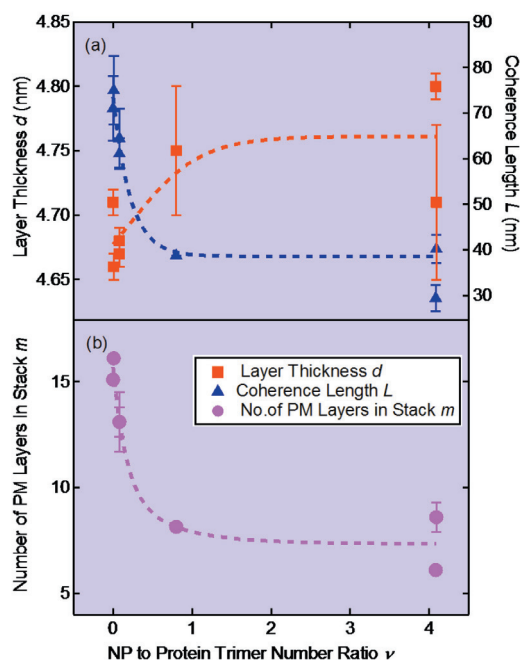


Fig. 10: (a) The PM layer thickness d (■; left axis) and the coherence length L (▲; right axis) in PM films with Fe_3O_4 NPs, plotted against the NP to PM trimer number ratio v . (b) Number of PM layers m in each multilayer stack (●) vs. v for Fe_3O_4 NPs added to the PM films using both CS and FP methods. The dashed curves are guides to the eye.

a similar effect, causing an increase in the disorder in the film structure, as assessed by the decreasing number of layers in the multilayer stack as the NP concentration increased (Fig. 10b).

Complementary UV-Visible spectroscopic measurements of the same films deposited on quartz showed that the conformation of the retinal residue within the protein was intact so that the proton pumping functionality of PM multilayers would be retained in all samples with added NPs. Subsequent atomic force microscopy measurements displayed NPs aggregated on top of the films, rather than becoming embedded into the films.

Our results show that the effects of NPs on the PM structure and functionality are subtle and complex. Also in the paper [4] we fully discuss the structural integrity of lipid-protein composite PM films against NP infiltration in terms of their high bending modulus as compared with that of fluid lipid bilayers.

- [1] L. Zhang *et al.*, J. Mat. Chem. 19, 1884 (2009).
- [2] R. Henderson, Ann. Rev. Biophys. Bioeng. 6, 87 (1977).
- [3] T. G. Dane *et al.*, Soft Matter 8, 2824 (2012).
- [4] J.M. Bulpett *et al.*, J. Mat. Chem. 22, 15635 (2012).

Using correlation functions to study non-equilibrium surface dynamics: a model study on ion eroded surfaces

O. Bikondoa, D. Carbone, V. Chamard and T.H. Metzger – for more information contact O. Bikondoa at XMaS-CRG Beamline, ESRF, B.P. 220, 38043 Grenoble cedex, France.

olier.bikondoa@esrf.fr

The erosive action of an ion beam on a semiconductor surface can lead to the formation of dotted or rippled patterns at the nanoscale. Visually, these patterns resemble those formed at the macroscale by wind erosion of sandy soils and indeed, the models to describe pattern formation on such different systems and length scales are similar [1]. However, the theoretical models to describe the time evolution of the erosion process are still debated. In general, the theoretical predictions have been qualitatively compared with microscopy or conventional (i.e. non-coherent) scattering measurements but due to the very special setups needed, only the latter can be applied in-situ and provide time-resolved information.

In some cases, the patterns reach a quasi-equilibrium state in which the ensemble averaged quantities, such as the mean distance between dots and ripples or the roughness, do not change anymore. However, the surface is still evolving due to erosion. Several theoretical models in the literature can predict similar behaviours for the evolution of ensemble averaged quantities. It is not possible therefore to determine which model is the correct one by comparing predictions with experimental data obtained with conventional scattering techniques. We show, based on calculations, that theoretical models predicting similar asymptotic behaviours of ensemble averaged quantities yield very different dynamic behaviours, that is, different behaviours of the local surface morphology evolution. Dynamical information can be obtained with coherent techniques such as X-ray photon correlation spectroscopy which are used to measure multi-time correlations (see Ref. [2] and references therein).

We have studied two equations proposed to describe ion beam sputtering at normal incidence (namely, the damped Kuramoto-Sivashinsky equation [3] and an equation proposed by Castro *et al.* [4]). We have numerically integrated the equations and calculated the two-time correlation functions for a set of parameters (Fig. 11). Both equations predict a saturation of the roughness but on the other hand they predict very

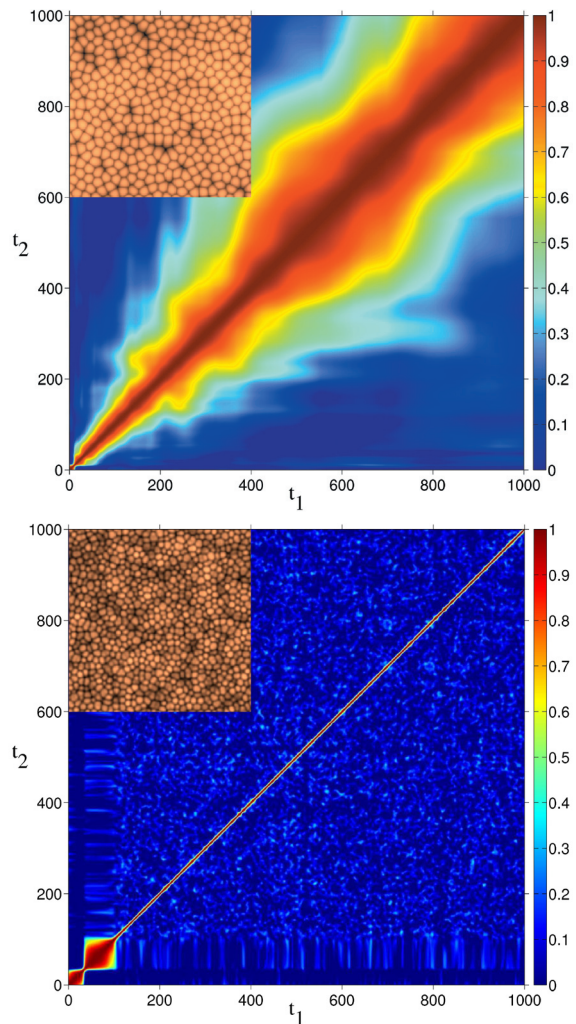


Fig. 11: Two-time correlation functions calculated for the equations proposed in Ref [3] (top) and Ref [4] for a specific set of parameters (see Ref. [2] for details). The insets show examples of surface topographies obtained by numerical integration of the equations, at $t=500$. The lateral dimensions of the insets can be rescaled arbitrarily.

different dynamical behaviours. In one case, the damped Kuramoto Sivashinsky equation predicts a system showing spatiotemporal chaos and stationary dynamics while the other equation shows non-equilibrium dynamics that slow down with time [2].

Our study demonstrates that the determination of two-time correlation functions using for example X-ray photon correlation spectroscopy can provide a unique way to discriminate between theoretical models describing pattern formation.

[1] R. Cuerno *et al.*, Nucl. Instr. Meth. B 269, 894 (2011).

[2] O. Bikondoa *et al.*, J. Phys.:Cond. Matter 24, 445006 (2012).

[3] S. Facsko *et al.*, Phys. Rev. B 64, 153412 (2004).

[4] M. Castro *et al.*, Phys. Rev. Lett. 94, 016102 (2005).

Guidelines

for beam-time applications

→ Beamline Operation

The XMaS beamline at the ESRF, which came into operation in April 1998, has some 174 days of beam time available each year for UK user experiments, after deducting time allocated for ESRF users, machine dedicated runs and maintenance days. During the year, two long shut-downs of the ESRF are planned: 4 weeks in winter and 4 weeks in summer. At the ESRF, beam is available for user experiments 24 hours a day.

→ Applications for Beam Time

Two proposal review rounds are held each year. **Deadlines for applications to make use of the mid-range facility (CRG) time are normally, 1st April and 1st October** for the scheduling periods August to end of February, and March to July, respectively. Applications for Beam Time must be submitted electronically following the successful model used by the ESRF. Please consult the instructions given in the ESRF web page:

www.esrf.eu

Follow the links: “User Portal” under “Quick Links”

Enter your surname and password
and select: “Proposals/Experiments”

Follow the instructions carefully – you must choose “CRG Proposal” and “XMAS-BM28” at the appropriate stage in the process. A detailed description of the process is always included in the reminder that is emailed to our users shortly before the deadline – for any problems contact L. Bouchenoire (boucheno@esrf.fr).

Technical specifications of the beamline and instrumentation available are described in the XMaS web page.

When preparing your application, please consider the following:

■ Access to the mid-range facility time is only for UK based researchers. Collaborations with EU and international colleagues are encouraged, but the proposal must be lead by a UK based principal investigator and it must be made clear how the collaborative research supports the UK science base. Applications without a robust link to the UK will be rejected and should instead be submitted directly to the ESRF.

■ All sections of the form must be filled in. Particular attention should be given to the safety aspects, and the name and characteristics of the substance completed

carefully. Experimental conditions requiring special safety precautions such as the use of electric fields, lasers, high pressure cells, dangerous substances, toxic substances and radioactive materials, must be clearly stated in the proposal. Moreover, any ancillary equipment supplied by the user must conform with the appropriate French regulations. Further information may be obtained from the ESRF Experimental Safety Officer, tel: +33 (0)4 76 88 23 69; fax: +33 (0)4 76 88 24 18.

■ Please indicate your date preferences, including any dates that you would be unable to attend if invited for an experiment. This will help us to produce a schedule that is satisfactory for all.

■ An experimental report on previous measurements must be submitted. **New applications will not be considered unless a report on previous work is submitted.** These also should be submitted electronically, following the ESRF model. The procedure for the submission follows that for the submission of proposals – again, follow the instructions in the ESRF’s web pages carefully. **Reports must be submitted within 6 months of the experiment.**

■ The XMaS beamline is available for one third of its operational time to the ESRF’s user community. Applications for beamtime within that quota should be made in the ESRF’s proposal round - **Note: their deadlines are earlier than for XMaS! - 1st March and 1st September.** Applications for the same experiment may be made both to XMaS directly and to the ESRF. Obviously, proposals successfully awarded beamtime by the ESRF will not then be given beamtime additionally in the XMaS allocation.

→ Assessment of Applications

The Peer Review Panel for the UK-CRG considers the proposals, grades them according to scientific excellence, adjusts the requested beam time if required, and recommends proposals to be allocated beam time on the beamline.

Proposals which are allocated beam time must in addition meet ESRF safety and XMaS technical feasibility requirements.

Following each meeting of the Peer Review Panel, proposers will be informed of the decisions taken and some feedback provided.



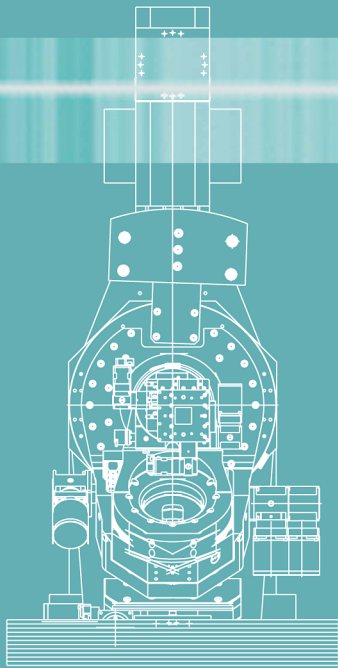
is an EPSRC sponsored project

XMaS, ESRF, 6 rue Jules Horowitz BP 220, 38043 Grenoble Cedex 9, France

Tel: +33 (0)4 76 88 25 80; Fax: +33 (0)4 76 88 24 55

web page : www.esrf.eu/UsersAndScience/Experiments/CRG/BM28/ – email: boucheno@esrf.fr

New: Modular Beam Conditioning Unit



- Beam Position and Intensity Monitor
- Slit Module
- Shutter Module
- Filter Module
- Protein Crystallography Unit

BCU 3100

We make the Best of your Beam

X-Ray Diffractometers
and Cameras

Multiaxis Goniometers
for X-Ray-, Synchrotron-
and Neutron Facilities

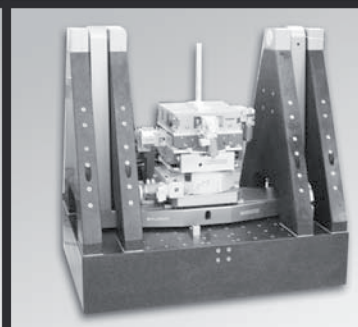
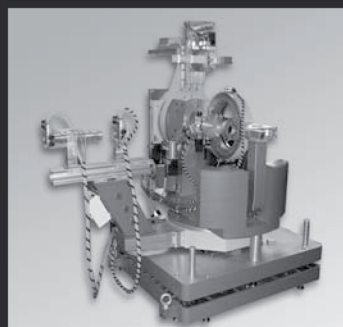
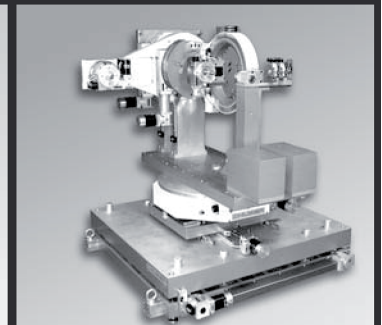
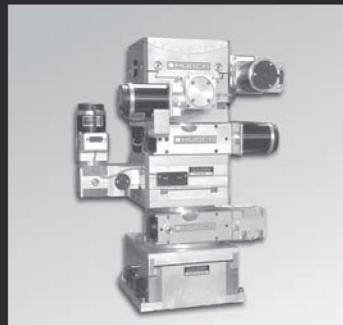
Monochromators

Positioning Devices
for Various Environments

Custom Built Instruments

Electronics

Accessories



HUBER Diffraktionstechnik
GmbH & Co. KG
Sommerstrasse 4
D-83253 Rimsting, Germany

www.xhuber.com
info@xhuber.com

HUBER
Diffraction and Positioning Equipment